# Physics-based Electrochemical Model of a Proton Exchange Membrane Water Electrolyzer

Nicolas Vignal 1,3, Zhongliang Li 1, Benoit Latour 3, Daniel Hissel 1,2

<sup>1</sup> Université Marie et Louis Pasteur, UTBM, CNRS, institut FEMTO-ST, F-90000 Belfort, France

<sup>2</sup> Institut Universitaire de France (IUF), France

<sup>3</sup> Research and Development Operations Department, Michelin Ladoux, Cébazat, France

Abstract— This article presents the electrochemical aspect of a multiphysics model for a 1 kW proton exchange membrane (PEM) water electrolyzer. The electrochemical sub-model is based on established equations, incorporating corrections to the standard electrochemical formula to enhance generalization across different temperatures. The model parameters affecting electrochemical performance are identified to better represent real physical processes. Validation is conducted using experimental data obtained under various inlet temperature conditions. The optimized model accurately predicts electrochemical behavior in the temperature range of 40°C to 70°C. These results demonstrate the model's capability to reflect temperature-dependent electrochemical processes.

#### I. INTRODUCTION

In the context of achieving carbon neutrality, the development of efficient and sustainable technologies to reduce the environmental impact of industries has gained significant attention. Hydrogen is widely seen as a key approach to addressing global warming and is already used in many industrial applications [1, 2, 3]. Due to its broad range of uses, transitioning to a hydrogen-based economy needs substantial advancements in the efficiency and sustainability of hydrogen production methods. To achieve carbon neutrality by 2050, France has committed to investing in hydrogen energy development, including the installation of at least 6.5 GW of electrolyzer capacity [4]. Similarly, the European Union aims to reach climate neutrality by 2050 through a series of actions, such as the Green Deal project [5].

One promising approach to large-scale hydrogen production is the direct coupling of water electrolyzers with intermittent renewable energy sources, such as wind and solar power. This integration enables the production of "green hydrogen," but it also presents challenges. High variability in the electrical current supplied by renewable sources can lead to premature aging of electrolyzers and increased overall system costs [6]. Among the various electrolyzer technologies, Proton Exchange Membrane (PEM) water electrolyzers are particularly suited for use with renewable energy sources due to their superior dynamic performance, wide operating range, compact design, and ability to produce high-purity hydrogen without the need for potassium hydroxide as an electrolyte [7, 8]. Other technologies, such as Alkaline, Solid-Oxide (SO), and Anion Exchange Membrane (AEM) electrolyzers, offer specific advantages but are presently less adaptable to fluctuating power inputs.

Physics-based models play a critical role in understanding and predicting the performance of electrolyzers under various operating conditions. For PEM electrolyzers, it is important to model power consumption as a function of time compared to hydrogen production to evaluate performance. Stack-level modeling, which considers the collective behavior of multiple cells, is preferred for its proximity to real-world operation. It enables researchers to numerically approximate system performance while isolating it from plant-level complexities.

Over the past decade, most PEM electrolyzer models have been empirical, semi-empirical, or analytical, with limited validation using experimental data [9, 10, 11]. Although several models, such as those developed by Agbli et al. [12], have provided valuable insights, advancements in PEM electrolyzer modeling have been relatively scarce since the last comprehensive review on the subject [10]. Existing models primarily focus on the cell level and attempt to couple different physical phenomena. When transitioning from cell-level to stack-level modeling, challenges such as parameter inhomogeneity and scaling effects further complicate the process [13].

The model proposed in this study builds upon the work of Agbli et al. [12] and incorporates corrections to electrochemical equations for modeling activation, ohmic, and diffusion losses. Unlike previous models, which assume symmetrical reactions with a charge transfer coefficient of 0.5 for both the anode and cathode, this study introduces a novel approach for identifying electrochemical parameters, including anode and cathode charge coefficients, using physics-based equations.

This article presents the electrochemical part of a multiphysics model applied to a dry cathode PEM electrolyzer stack with experimental validation performed on a 10-cell stack. The use of a short stack provides a balance between experimental feasibility and the complexity of scaling effects. The proposed modeling approach integrates cell-level physics with stack-level calibration using real experimental data. The model accurately predicts system behavior under various operating conditions, including dynamic load changes, and highlights key physical phenomena that influence performance. Furthermore, the study discusses the model's limitations, such as challenges in scaling from cell-level to stack-level modeling. These analyses aim to identify areas for improvement and provide a comprehensive understanding of the model's strengths and weaknesses. By bridging the gap between cell-level and stack-level modeling, this study contributes to the development of more robust and accurate models for PEM electrolyzers. Such advancements are essential for improving hydrogen production systems and supporting the transition to a sustainable hydrogen-based economy.

To accurately model PEM water electrolyzers, it is essential to account for the electrochemical processes that govern their operation. These processes include activation, ohmic, and diffusion losses, which collectively impact the system's efficiency and performance. A precise understanding of these phenomena is necessary to develop models capable of predicting system behavior under varying operating conditions. By incorporating corrections to electrochemical equations and finding key parameters such as charge transfer coefficients at the anode and cathode, this study finally aims to enhance the reliability and applicability of PEM electrolyzer models. This refined electrochemical model serves as the foundation for the Multiphysics modeling approach.

The paper is organized as follows: Section II presents the electrochemical modelling of the PEM water electrolyzer, detailing the key hypotheses in Part A, the formulation of activation, ohmic, and diffusion losses in Part B, and the detail model of electrochemical parameter to take temperature dependence into account in Part C. Section III describes the identification and validation of these parameters via a geneticalgorithm—based estimation routine, and Section IV draws the conclusions and outlines perspectives for further improvement.

#### II. MODELING OF PEM WATER ELECTROLYZER

## A. Modelling hypothesis

Developing a physics-based model involves carefully considering the physical limits that affect the system. Various hypotheses have been proposed to accurately model the operation of the stack by considering different physical phenomena:

- Cells are assumed to be identical, independent, and isolated.
- Mechanical motion and electromagnetic forces are neglected.
- Current density is considered uniform across the entire active area of the electrodes.
- Auxiliary components, such as cooling and gas handling systems, are not modeled, and their impact on system behavior is assumed to be negligible.
- The cathode is modeled as a dry system, with no liquid water present at the cathode side.
- The anode operates at atmospheric pressure, simplifying pressure-dependent phenomena.
- Temperature is considered uniform throughout the system.

This model achieves high accuracy in simulating the responses of the electrolyzer within a temperature range of 30 °C to 70 °C. These hypotheses provide a balance between simplifying assumptions and physical fidelity.

#### B. Electrochemical modeling

Electrochemical physics describes chemical phenomena coupled with electrical energy. This enables the quantification of voltage losses and the assessment of system performance. The Gibbs free energy, a key thermodynamic quantity, is calculated using the following equation:

$$\Delta G = \Delta H - T \Delta S \tag{1}$$

where  $\Delta G$  is the free Gibbs energy  $[J \cdot mol^{-1}]$ ,  $\Delta H$  is the standard enthalpy  $[J \cdot mol^{-1}]$ , T is the temperature [K] and  $\Delta S$  is the entropy difference  $[J \cdot mol^{-1} \cdot K^{-1}]$ 

The reversible voltage corresponds to the minimum voltage required for the electrolysis reaction to occur under ideal conditions and is defined as

$$V_{rev} = \left| \frac{\Delta G}{n \cdot F} \right| \tag{2}$$

with n the number of electrons exchanged, F the Faraday constant  $[C \cdot mol^{-1}]$ ,  $V_{rev}$  is the reversible voltage [V].

At standard conditions at 25°C and 1 atm, the Gibbs free energy is 237  $kJ \cdot mol^{-1}$  and the minimum dissociation voltage of water is 1.23 V. A temperature-dependent expression for the reversible voltage was proposed by Harrison et al. [13], based on thermodynamic values:

$$V_{rev} = 1.229 - 0.9 \cdot 10^{-3} \cdot (T - 298) \tag{3}$$

with T is stack temperature [K].

As the system is not ideal, the reversible voltage is corrected using the Nernst equation [14], which accounts for pressure differences to calculate the true open-circuit voltage (OCV):

$$V^{0} = \left[ V_{rev} + \frac{R \cdot T}{n \cdot F} \cdot log \left( \frac{\frac{P_{H_2}}{P_{cat,0}} \cdot \sqrt{\frac{P_{O_2}}{P_{an,0}}}}{a_{H_2O}} \right) \right] \cdot N_{cell} \quad (4)$$

with R is ideal gas constant  $[J \cdot K^{-1} \cdot mol^{-1}]$ ,  $P_{cat,0}$  reference fluid pressure at the cathode [Bar],  $P_{an,0}$  reference fluid pressure at the anode [Bar],  $p_{H_2}$  partial pressure of hydrogen at the cathode [Bar],  $p_{O_2}$  partial pressure of oxygen at the anode [Bar],  $a_{H_2O}$  is activity of water [1].

Voltage losses beyond the reversible voltage, called overpotentials, must be overcome for the electrolysis reaction to proceed. The main overpotentials include activation, ohmic, and diffusion losses.

The activation overpotential accounts for the energy barrier associated with the electrochemical reactions. Assuming uniform current density across the electrodes, the activation losses at the anode and cathode are given by:

$$\eta_{act,an} = \frac{R \cdot T}{n \cdot \alpha_a \cdot F} \cdot asinh\left(\frac{j}{2 \cdot j_{0,a}}\right) \cdot N_{cell}$$
 (5)

$$\eta_{act,cat} = \frac{R \cdot T}{n \cdot \alpha_c \cdot F} \cdot asinh\left(\frac{j}{2 \cdot j_{0,c}}\right) \cdot N_{cell}$$
(6)

with  $\alpha_c$  cathode charge transfer coefficient [1],  $\alpha_a$  anode charge transfer coefficient [1],  $j_{0,a}$  anode exchange current density  $[A \cdot cm^{-2}] j_{0,c}$  cathode exchange current density  $[A \cdot cm^{-2}]$ , j current density  $[A \cdot cm^{-2}]$ ,  $N_{cell}$  number of stack cells

The total activation losses correspond to the addition of anodic and cathodic activation losses, resulting in the following value:

$$\eta_{act} = \eta_{act,an} + \eta_{act,cat} \tag{7}$$

with  $\eta_{act}$  activation losses [V].

Ohmic resistance losses represent the resistance of the system to ionic and electronic transport in the system, with the membrane resistance being the dominant factor. Using Ohm's law, the ohmic losses are expressed as:

$$\eta_{ohm} = R_e \cdot j \cdot N_{cell} = \frac{\phi}{\sigma_m} \cdot j \cdot N_{cell}$$
 (8)

with  $R_e$  membrane resistance  $[\Omega]$ ,  $\phi$  membrane thickness [m] and  $\sigma_m$  membrane conductivity  $[S \cdot m^{-1}]$ .

The concentration overpotential, or diffusion overpotential, arises from gas transport limitations within the cell. This effect is often negligible under low current densities, where ohmic and activation losses dominate. A derivative of the Nernst equation is used to quantify the diffusion overpotential:

$$\eta_{conc} = \left(\frac{R \cdot T}{4 \cdot F} \cdot l \, n \, \frac{C_{O_2,mem}}{C_{O_2,mem}^0} + \frac{R \cdot T}{2 \cdot F} \cdot l \, n \, \frac{C_{H_2,mem}}{C_{H_2,mem}^0}\right) \cdot N_{cell}(9)$$

with  $C_{O_2,mem}$  oxygen concentration at membrane — anode interface  $[mol \cdot l^{-1}]$ ,  $C_{O_2,mem}^0$  oxygen reference concentration at membrane — anode interface  $[mol \cdot l^{-1}]$ ,  $C_{H_2,mem}$  hydrogen concentration at membrane — cathode interface  $[mol \cdot l^{-1}]$ ,  $C_{H_2,mem}^0$  hydrogen reference concentration at membrane — cathode interface  $[mol \cdot l^{-1}]$ .

The total voltage of the stack, as a function of the input current, is calculated by summing the reversible voltage and all losses.

$$U_{stack}(I,T) = V^{0}(T) + \eta_{act}(I,T) + \eta_{conc}(I,T) + \eta_{ohm}(I,T)$$

$$(10)$$

The determination of activation overpotentials and ohmic losses requires a detailed understanding of the parameters that influence them, such as the anode and cathode charge transfer coefficients  $(\alpha_{an}, \alpha_{cat})$ , the exchange current densities  $(j_{0,an}, j_{0,cat})$ , and the membrane conductivity  $(\sigma_m)$ . These parameters are tied to the system's electrochemical physics and depend on temperature, pressure, and material properties. The following section focuses on deriving and refining these parameters based on physical principles.

## C. Electrochemical parameters modeling

The influence of operating conditions on electrochemical parameters can be described using physical equations. Specifically, the exchange current density  $(j_{0,an},j_{0,cat})$ , charge transfer coefficient  $(\alpha_{an}, \alpha_{cat})$ , and membrane conductivity  $(\sigma_m)$  are highly dependent on factors such as pressure, temperature, and concentration:

$$i_0 = f(P, T) \tag{11}$$

$$\alpha = f(P, T, C_i) \tag{12}$$

$$\sigma_m = f(T, HR) \tag{13}$$

with P is partial pressure of hydrogen or oxygen at electrode interface [bar], T temperature of electrode [K],  $C_i$ 

concentration at electrode interface  $[mol \cdot l^{-1}]$  and HR is relative humidity of the membrane [1].

In this study, certain assumptions simplify the model and reduce its complexity. Experimental bench data confirm that the system operates under atmospheric pressure. Although technology theoretically prevents liquid water from forming at the cathode side, hydraulic pressure causes water to permeate the membrane alongside H<sup>+</sup> protons. As a result, the membrane's hydration level is assumed to remain at nearly maximum.

The concentration of species at the electrode interface is difficult to measure at the system level under operating conditions without significantly impacting the system. To address this, it is assumed that pressure variations and species concentration have a negligible effect on the model parameters governing electrochemical activation and ohmic losses. These simplifications reduce the complexity of the parameter space, allowing the model to focus on temperature as the dominant factor influencing key parameters such as  $j_{0,an}$ ,  $j_{0,cat}$ ,  $\alpha_{an}$ ,  $\alpha_{cat}$  and  $\sigma$ .

Temperature is a critical factor affecting the performance of electrochemical systems. For many physical parameters, such as exchange current density and conductivity, the temperature dependence can be modeled using an Arrhenius-type equation. This approach has been extensively applied to describe the oxygen evolution reaction (OER) and hydrogen evolution reaction (HER) kinetics. For instance, Moore et al. [15] derived the following equation for the OER. The parameters for the OER and HER are highly dependent on the electrode materials used, such as platinum and iridium oxide in PEM water electrolyzers. To generalize the relationship and account for variations in electrode materials, the exchange current density is expressed as:

$$j_{0,an} = \gamma_a \cdot \exp\left(-\frac{E_a}{R \cdot T}\right) \tag{14}$$

$$j_{0,cat} = \gamma_c \cdot \exp\left(-\frac{E_c}{R \cdot T}\right) \tag{15}$$

with  $E_a$  and  $E_c$  are defined as activation energy for the electrode reaction in  $[J \cdot mol^{-1}]$ ,  $\gamma_a$  and  $\gamma_c$  the pre-exponential factor [1].

Based on traditional modeling of ohmic conductivity of the membrane in fuel cell, the conductivity of membrane parameter is modeled as a function of temperature using an Arrhenius-type equation:

$$\sigma_m(T) = \gamma_m \cdot \exp\left(-\frac{E_{H^+}}{R \cdot T}\right)$$
 (16)

with  $E_{H^+}$  is a parameter that represents the activation energy for proton transport in the membrane  $[J \cdot mol^{-1}]$ ,  $\gamma_m$  the pre-exponential factor [1].

Other parameters exhibit simpler relationships with temperature. In this model, it is assumed that the charge transfer coefficient  $(\alpha_{an}, \alpha_{cat})$  is often modeled as a linear function of temperature, with the influence of pressure considered negligible under typical operating conditions. Tijani et al. [18] demonstrated that the dependence of  $\alpha$  on

pressure is minimal, allowing the relationship with temperature to be expressed as:

$$\alpha_{an}(T) = \phi_a \cdot T + \beta_a \tag{17}$$

$$\alpha_{cat}(T) = \phi_c \cdot T + \beta_c \tag{18}$$

with  $\phi_a$ ,  $\phi_c$ ,  $\beta_a$  and  $\beta_c$  are material-specific coefficients derived from experimental data.

The relationships between electrochemical parameters established propose a more detailed model for electrochemical dependence of some materials in the system. The next step involves parameter identification using experimental data. This step ensures that the model accurately captures the physical behavior of the system by estimating key parameters such as  $\alpha_{an}$ ,  $\alpha_{cat}$ ,  $j_{0,an}$ ,  $j_{0,cat}$  and  $\sigma_m$  under realistic operating conditions.

#### III. IDENTIFICATION AND VALIDATION

# A. Parameter identification using genetic algorithm

The system studied is a PEM electrolyzer stack manufactured by Leancat (LCWE-25-10 model) with a nominal power of 1 kW, a current range of 15 to 50 A, a hydrogen operating pressure of 0 to 20 barg, an operating temperature range of 30 to 70°C, and an active surface area of 25 cm<sup>2</sup>. Characterization was performed using a specific current profile to identify activation and ohmic resistance losses, with data acquired at 40°C, 45°C, 50°C, 60°C, and 70°C under atmospheric pressure. The current profile ranged from 0 to 50 A, corresponding to current densities from 0 to 2  $A \cdot cm^{-2}$ . Voltage, current, and temperature measurements were logged every 100 milliseconds using synchronized, highprecision acquisition systems, while a buffer tank ensured precise temperature control. Data analysis shows minimal voltage differences between 40°C and 50°C in the activation region due to limited heat generation. Higher temperatures reduce voltage demand, confirming that increased operating temperature improves efficiency by lowering activation losses.

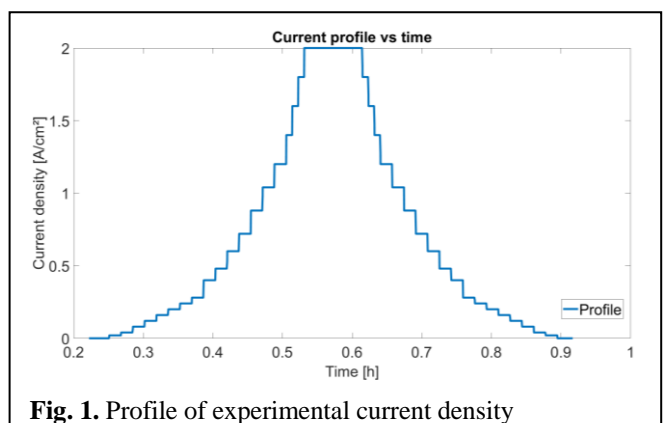


Figure 1 depicts the profile of current density as a function of time, measured in seconds. Initially, the current density rises gradually in discrete steps until it reaches approximately  $2 A \cdot cm^{-2}$  and the current density decreases in a similar stepwise manner, returning to zero. This profile aims to study the electrochemical response of voltage with step rise and decrease.

The minimal set of inputs for the model is designed with an industrial perspective in mind, considering systems equipped with only a limited number of measurement sensors, which are the current profile supplied to the system and the water temperature at the stack inlet. These constraints are used to identify model parameters and estimate their values under the given operating conditions. To further refine the coefficients derived from the model equations, a genetic algorithm (GA) is employed. GA offers advantages over traditional optimization methods, such as the least mean square method, as it is less prone to becoming trapped in local optima [16, 17]. The optimization objective function minimizes the error between the experimentally measured voltage and the voltage predicted by the model. The root mean square error (RMSE) is used as the objective function, as it is widely applied in regression analysis for its ability to evaluate prediction accuracy.

In addition to minimizing the RMSE, physical constraints are imposed using a penalty function. For each constraint violation, a penalty is added to the total error, ensuring that the optimization results respect the physical principles of the system. The total cost function is expressed as follows:

$$L(x) = RMSE(x) + r \cdot p_x \tag{19}$$

where L(x) is the objective function, r is the penalty factor and  $p_x$  is the distance between the estimated parameter value and its upper or lower bounds.

Bounds are chosen based on experimental observations and prior knowledge, ensuring the parameters remain physically meaningful within the range of operating conditions. For each parameter, there were as follows:

$$0.1 < \alpha_{an} < 0.3$$
 (20)

$$0.6 < \alpha_{cat} < 1.1$$
 (21)

$$1 \cdot 10^{-12} \text{A} \cdot \text{cm}^{-2} < j_{0,an} < 1 \cdot 10^{-8} \,\text{A} \cdot \text{cm}^{-2}$$
 (22)

$$1 \cdot 10^{-3} \text{A} \cdot \text{cm}^{-2} < j_{0,cat} < 1 \cdot 10^{-1} \text{ A} \cdot \text{cm}^{-2}$$
 (23)

$$10 \text{ mS} \cdot \text{cm}^{-1} < \sigma_{cell} < 100 \text{ mS} \cdot \text{cm}^{-1}$$
 (24)

For this optimization problem, the GA configuration includes a population of 100 individuals and is considered to provide a sufficiently diverse sample of potential solutions. This ensures that the search space is adequately covered, while remaining computationally tractable. Each individual is represented by a vector of 10 genes, where each gene corresponds to a specific electrochemical parameter. This encapsulates the complex physical characteristics of the system. The population evolves over 500 generations, which allows the algorithm many opportunities to iteratively refine solutions through selection, crossover, and mutation. This increases the likelihood of converging on a global optimum while mitigating the risk of premature convergence on local optima. In each generation, 10 parents are selected using a tournament selection strategy. The remaining individuals, despite not being selected as direct contributors to the subsequent generation, nevertheless exert an influence on the competitive dynamics by participating in tournaments and by ensuring the maintenance of overall genetic diversity. The tournament strategy compares a subset of individuals and selects the best among them. This strategy balances exploration and exploitation of the search space. The crossover operation is performed using a single-point method, and mutations are applied adaptively. Adaptive mutations are defined as the dynamic adjustment of the mutation rate based on the current state of the population. During periods of stagnation or reduced diversity, the mutation rate is dynamically increased to promote exploration, while during periods of steady convergence, it is decreased to refine optimal solutions. To retain high-quality solutions, elitism is implemented, preserving the two best individuals in each generation. The initial population is either explicitly provided or randomly generated within the predefined parameter bounds.

The optimization yields a root mean squared error (RMSE) for training data of 0.093 V at 40 °C and 0.100 V at 60 °C. For the validation data set, the results are 0.148 V at 50 °C and 0.151 V at 70 °C (see figure 3). The small difference between training and validation errors indicates a robust model, with low prediction errors under these conditions. The value of each coefficient from 40 to 80 °C remains within the bounds. The set of parameters obtained is as follows:  $\phi_a = 9.26 \cdot 10^{-4}, \ \beta_a = 5.82 \cdot 10^{-1}, \ \phi_c = 9.99 \cdot 10^{-4}, \ \beta_c = 1.36 \cdot 10^{-2}, \ \gamma_a = 9.98 \cdot 10^{-7}, \ E_a = 1.00 \cdot 10^4, \ \gamma_c = 9.98, \ E_c = 1.32 \cdot 10^4, \ \gamma_m = 6.34 \cdot 10^{-1}, \ E_{H^+} = 5.99 \cdot 10^3.$ 

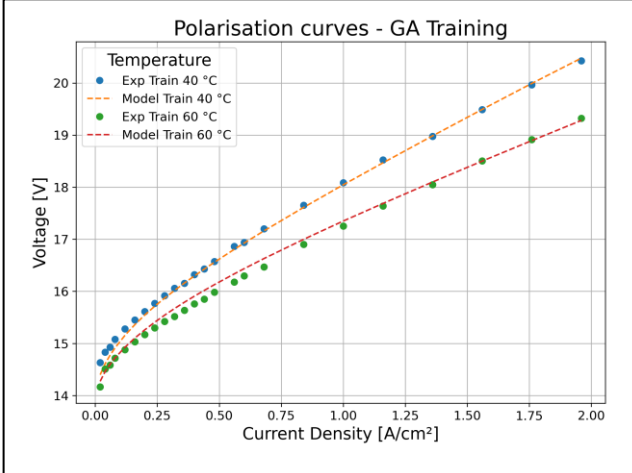


**Fig. 2.** Results with genetic algorithm estimations of coefficients at different temperatures.

As shown in Figure 2, the results indicate excellent parameter estimation, with a mean error RMSE for the four curves of 0.123 V between the experimental and modeled data points. The results confirm that the identified parameters accurately capture the system's behavior, with their values being consistent and physically meaningful under all conditions evaluated.

With the identified parameter set validated against experimental data, the next step involves analyzing the impact of these parameters on the system's performance. This includes investigating their temperature dependence and physical significance to ensure the model aligns with the underlying electrochemical principles of PEM electrolyzers.

After identifying the optimal electrochemical parameters using the genetic algorithm, the model is validated by comparing its predictions to experimental data obtained under various operating conditions. This step ensures that the identified parameters accurately capture the electrochemical behavior of the PEM electrolyzer stack. Validation also confirms the model's consistency with physical principles and its reliability within the defined operating range.

# B. Validation part

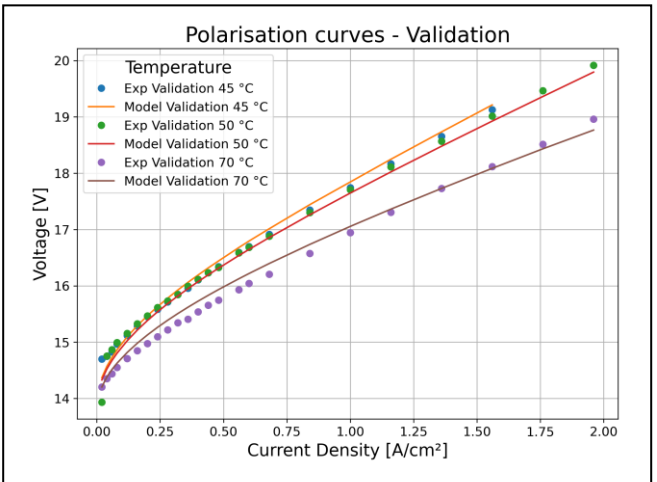


**Fig. 3.** Validation result with genetic algorithm at different temperatures.

Model validation was conducted using additional data acquired at 45°C. The simulation results (Fig. 4) show a high level of accuracy, with errors below 5%. At 45°C and 1 bar pressure, the model yielded an MSE of 0.003 V² and an RMSE of 56 mV, demonstrating the reliability of the model's assumptions, computational algorithms, and parameter estimation. Prediction error is remarkably low for a stack of 10 cells. The model is thus validated over the full operating range of 40°C to 70°C.

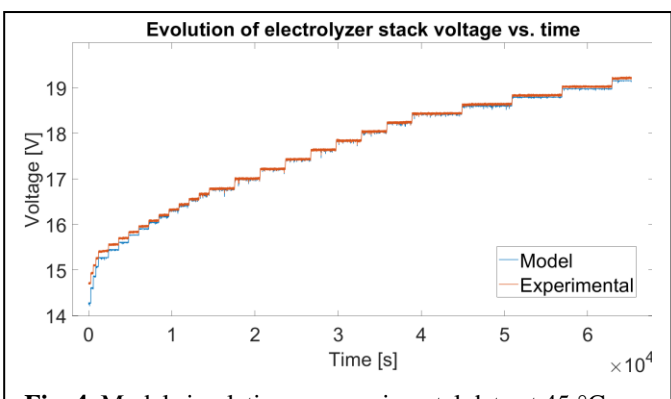


Fig. 4. Model simulation vs experimental data at 45 °C.

At low current densities ( $< 0.5~A \cdot cm^{-2}$ ), the model accurately captures the steep increase in voltage caused by activation losses. The Butler-Volmer equation effectively represents the electrochemical reactions in this region, with the charge transfer coefficients ( $\alpha_{an}$ ,  $\alpha_{cat}$ ) and the exchange current densities ( $j_{0,an}$ ,  $j_{0,cat}$ ) effectively characterize the electrochemical kinetics in this region. From the graphic, this region is observed at voltage between 14 and 16 V, where the activation overvoltage is the most important. Notably, these parameters exhibit significant temperature dependence, an

increase in temperature reduces the activation barrier. thereby enhancing the exchange current densities in accordance with Arrhenius behavior. The close agreement between simulated and experimental results in this range confirms the model's ability to characterize electrochemical kinetics. In the intermediate current density range  $(0.5 - 2~A \cdot cm^{-2})$ , the voltage increases linearly with current density, a trend characteristic of ohmic losses. Furthermore, the temperature dependence of ionic conductivity  $(\sigma_m)$ , wherein higher temperatures generally improve ion mobility, is accurately integrated.

During validation, both ascending and descending current profiles were tested. The electrolyzer exhibits hysteresis due to differing system conditions when the current is increased versus decreased. To account for this, the experimental setup included a rising and then a falling current profile, and the voltage values at identical current steps were averaged to precisely characterize hysteresis effects across the operating range. The observed voltage hysteresis is primarily attributed to the dynamics of reactive species and the stack temperature which is higher in the falling part. This approach provides a robust quantitative measure of the hysteresis phenomena impacting electrochemical performance.

The strong correlation between the model predictions and experimental data confirms that the model accurately captures the key electrochemical processes within the PEM electrolyzer stack. This validation establishes confidence in the model's capability to simulate stack performance, enabling its application for further analysis. Recognizing the limitations of this study is essential for assessing the potential restrictions on the generalizability and practical applicability of its findings.

## IV. CONCLUSION

This study presents a validated precise electrochemical model for a PEM electrolyzer stack, capable of accurately predicting system performance across an operating range of 40°C to 70°C. By integrating electrochemical kinetics, ionic conductivity, and activation losses into the model, the simulation results demonstrate strong agreement with experimental data, with average errors below 5%. The use of genetic algorithms for parameter identification has proven effectiveness in optimizing model coefficients, ensuring that the results align with physical principles.

This work provides a reliable and versatile tool for analyzing and optimizing PEM electrolyzer stacks. The model can serve as a foundation for future studies, enabling researchers to explore the impact of operating conditions on system performance. In an industrial context, this model could support the development of more efficient hydrogen production systems by providing insights into key factors influencing efficiency and durability.

### ACKNOWLEDGMENT

This work was supported by EIPHI Graduate School (ANR-17-EURE-0002), Michelin, and Region Bourgogne Franche-Comté.

#### REFERENCES

- [1] J. O. Abe, A. P. Popoola, E. Ajenifuja and O. M. Popoola, "Hydrogen energy, economy and storage: Review and recommendation," International Journal of Hydrogen Energy, vol. 44, no. 29, pp. 15072-15086, 2019.
- [2] A. Midilli, H. Kucuk, M. E. Topal, U. Akbulut and I. Dincer, A comprehensive review on hydrogen production from coal gasification: Challenges and Opportunities, vol. 46, Pergamon, 2021, pp. 25385-25412.
- [3] M. A. Pellow, C. J. Emmott, C. J. Barnhart and S. M. Benson, "Hydrogen or batteries for grid storage? A net energy analysis," Energy and Environmental Science, vol. 8, no. 7, pp. 1938-1952, 2015.
- [4] "Stratégie nationale pour le développement de l'hydrogène décarboné en France," 8 Septembre 2020. [Online]. Available: https://www.economie.gouv.fr/presentation-strategie-nationaledeveloppement-hydrogene-decarbone-france#. [Accessed 4 avril 2024].
- [5] "2050 long-term strategy," European Commission, mars 2020.
   [Online]. Available: https://climate.ec.europa.eu/eu-action/climate-strategies-targets/2050-long-term-strategy\_en. [Accessed 17 décembre 2024].
- [6] A. Weiß, A. Siebel, M. Bernt, T.-H. Shen, V. Tileli and H. A. Gasteiger, "Impact of Intermittent Operation on Lifetime and Performance of a PEM Water Electrolyzer," Journal of The Electrochemical Society, vol. 166, no. 8, pp. F487-F497, 2019.
- [7] Q. Feng, X. Z. Yuan, G. Liu, B. Wei, Z. Zhang, H. Li and H. Wang, "A review of proton exchange membrane water electrolysis on degradation mechanisms and mitigation strategies," Journal of Power Sources, vol. 366, pp. 33-55, 2017.
- [8] M. El-Shafie, "Hydrogen production by water electrolysis technologies: A review," Results in Engineering, vol. 20, p. 101426, 2023.
- [9] D. Falcão and A. Pinto, "A review on PEM electrolyzer modelling: Guidelines for beginners," Journal of Cleaner Production, vol. 261, p. 121184, 2020.
- [10] H. Marefatjouikilevaee, F. Auger and J.-C. Olivier, "Static and Dynamic Electrical Models of Proton Exchange Membrane Electrolysers: A Comprehensive Review," 2023. [Online].
- [11] A. Arsad, M. Hannan, A. Q. Al-Shetwi, R. Begum, M. Hossain, P. J. Ker and T. I. Mahlia, "Hydrogen electrolyser technologies and their modelling for sustainable energy production: A comprehensive review and suggestions," 2023. [Online].
- [12] K. S. Agbli, M. C. Péra, D. Hissel, O. Rallires, C. Turpin and I. Doumbia, "Multiphysics simulation of a PEM electrolyser: Energetic Macroscopic Representation approach," International Journal of Hydrogen Energy, vol. 36, no. 2, pp. 1382-1398, 2011.
- [13] K. W. Harrison, E. Hernández-Pacheco, M. Mann and H. Salehfar, Semiempirical Model for Determining PEM Electrolyzer Stack Characteristics, Journal of Fuel Cell Science and Technology, vol. 3, 2006, pp. 220-223.
- [14] L. Järvinen, P. Puranen, A. Kosonen, V. Ruuskanen, J. Ahola, P. Kauranen, M. Hehemann, Automized parametrization of PEM and alkaline water electrolyzer polarisation curves, International Journal of Hydrogen Energy, Vol. 47, pp. 31985-32003, 2022
- [15] M. Moore, P. Wardlaw, P. Dobson, J. J. Boisvert, A. Putz, R. J. Spiteri and M. Secanell, "Understanding the Effect of Kinetic and Mass Transport Processes in Cathode Agglomerates," Journal of The Electrochemical Society, vol. 161, no. 8, pp. E3125-E3137, 2014.
- [16] B. Alhijawi and A. Awajan, Genetic algorithms: theory, genetic operators, solutions, and applications, vol. 17, 2023, pp. 1245-1256.
- [17] S. Katoch, S. S. Chauhan and V. Kumar, A review on genetic algorithm: past, present, and future, vol. 80, 2021, pp. 8091-8126.
- [18] A. S. Tijani, N. A. Binti Kamarudin and F. A. Binti Mazlan, "Investigation of the effect of charge transfer coefficient (CTC) on the operating voltage of polymer electrolyte membrane (PEM) electrolyzer," International Journal of Hydrogen Energy, vol. 43, no. 19, pp. 9119-9132, 2018.